European Review for Medical and Pharmacological Sciences 2021; 25: 4714-4728

One gut microbiota, *Fusobacterium nucleatum* aggravates Neonatal necrotizing enterocolitis by induction of IRF5 expression through lncRNA ENO1-IT1/miR-22-3p axis

J.-C. LIN[1], X.-Y. MA[2], J.-Y. LIU[3], Y.-Z. LUO[1], L. LIN[1], L.-Y. ZHANG[1]

[1]Department of Neonatology, Affiliated Fuzhou Children Hospital of Fujian Medical University, Gulou District, Fuzhou, Fujian, China
[2]Department of Neonatology, Fuzhou Children Hospital of Fujian province, Fuzhou, Fujian, China
[3]Fujian medical university, Fuzhou, Fujian, China

Jincai Lin and Xiaoying Ma contributed equally to this work

Abstract. – OBJECTIVE: We explored the effects of Fusobacterium nucleatum (*F. nucleatum*) in Neonatal necrotizing enterocolitis (NEC) and its possible mechanism.

MATERIALS AND METHODS: Patients with Neonatal NEC and normal healthy volunteers were collected for this study. Neonatal mice were administered with LPS and then exposed to hypoxia as a mice model of NEC. THP-1 cells were stimulated with LPS as an *in vitro* model of NEC.

RESULTS: We have demonstrated *F. nucleatum* abundance correlated with patients with Neonatal NEC or mice with Neonatal NEC. Furthermore, *F. nucleatum* stimulated colitis and increased inflammation in mice and *in vitro* models. LncRNA ENO1-IT1 was an important target for *F. nucleatum* in NEC-inflammation. MiR-22-3p was a target gene of *F. nucleatum* in NEC via LncRNA ENO1-IT1. Next, IRF5 was a target gene of miR-22-3p in the function of *F. nucleatum* in NEC via LncRNA ENO1-IT1. Silencing IRF5 or over-expressing miR-22-3p relieved the role of lncRNA ENO1-IT1 on inflammation in NEC via CD206 and CD86 expression.

CONCLUSIONS: Taken together, these results demonstrate that *F. nucleatum* is mechanically, biologically and clinically connected to NEC. LncRNA ENO1-IT1 may be important targets for *F. nucleatum* in NEC-inflammation, and a meaningful in treating patients with Neonatal NEC with elevated *F. nucleatum*.

Key Words:
Gut microbiota, *Fusobacterium nucleatum*, Neonatal necrotizing enterocolitis, MiR-22-3p, ENO1-IT1.

Introduction

Neonatal necrotizing enterocolitis (NEC) is an acquired disease, which is common as a digestive system disease in newborns, seriously threatening the life safety of children[1]. The epidemiological reports on NEC vary greatly from country to country[2]. The incidence of NEC in live births abroad is reported to range from 0.1% to 0.3%, accounting for 2% to 5% of inpatients in neonatal critical care unit (NICU)[2]. 85% of NEC patients are premature infants, while late preterm infants and term infants account for only 7% to 15%. The incidence of NEC in very low birth weight (VLBW) infants is approximately 7%, and the incidence is negatively correlated with gestational age[3]. Studies have shown that the incidence of NEC of preterm infants at 22-28 weeks of gestational age is the highest (11%)[3].

Some studies[4,5] have reported that the application of probiotics can cause fungemia, bacteremia and sepsis; however, children treated with probiotics all have digestive system complications. The reason is that the bacterial translocation occurs easily after the intestinal mucosal barrier is destroyed, which causes bacteremia after entering the intestinal wall into the blood, further aggravating intestinal mucosal damage and systemic inflammation[6]. The application of probiotics can decrease the risk of NEC in premature infants. However, there is currently no definite evidence revealing the direct relationship between the improved clinical symptoms and the improvement of the microecological flora structure by probiotics[6,7].

The progress of genomics has revealed that most of the transcripts of human genes are microRNA and lncRNA[8]. LncRNA, as a mechanism of transcription regulation, plays a key role

Corresponding Author: Liyan Zhang, MD; e-mail: Zhangliyan2332@163.com

in regulating gene expression, which has been confirmed to be involved in various physiological and pathological processes[9-11]. Multiple studies[12-14] have confirmed that apart from catalyzing the conversion between PGA and PEP, ENO-1 also plays an important role in multiple biological processes, including tumorigenesis and tumor development, apoptosis, plasminogen activation and plasmin activity, myogenesis and muscle regeneration, etc. We explored the effects of Fusobacterium nucleatum (*F. nucleatum*) in Neonatal necrotizing enterocolitis (NEC) and its possible mechanism.

Materials and Methods

Clinical Research Model

30 patients with Neonatal NEC and 30 normal volunteers were collected from Affiliated Fuzhou Children Hospital of Fujian Medical University. Intestinal contents and serum were collected and saved at -80°C. This experiment was performed in accordance with the Guide for the Care and Use of US National Institutes of Health. Experimental protocols were approved by the Affiliated Fuzhou Children Hospital of Fujian Medical University. Each patient provided their written informed consent for study participation. The enrollment and selection of inclusion in NEC neonatal patients: clinical evidence of perforation in the joint opinion by surgeon and the neonatologist; age < 34 weeks; birth weight, <1500 g; evidence of intestinal perforation: free intraperitoneal air on an abdominal radiograph (96 infants); stool, bile, or pus found at paracentesis.

The enrollment and selection of exclusion in NEC neonatal patients: bilateral grade IV intraventricular hemorrhage (i.e., severe intraventricular hemorrhage); previous abdominal operation; infants with gastrointestinal anomalies.

Bacterial Strains and Detection of Bacterial Abundance

Fusobacterium nucleatum, Enterotoxigenic Bacteroides fragilis, Peptostreptococcus anaerobius, Parvimonas micra and *Prevotella intermedia* were purchased from American Type Culture Collection (ATCC, Manassas, VA, USA). FFPE colon tissue was used to extract genomic DNA (gDNA) with QIAamp DNA FFPE Tissue Kit (QIAGEN, Hilden, Germany). gDNA was subjected detecting the 16S ribosome genes using real-time PCR.

Animals Model

Mice (C57BL/6) were performed in accordance with the Guide for the Care and Use of Laboratory Animals published by the US National Institutes of Health. C57BL/6 male mice were obtained from the Model Animal Research Center of Nanjing University (Nanjing, China). All aspects of the animal care and experimental protocols were approved by the Affiliated Fuzhou Children Hospital of Fujian Medical University. Committee on Animal Care.

A total of 76 newborn male (C57BL/6, weight 2-4 g) and female C57BL/6 mice (8 weeks old, weight 20-22 g) placed into an incubator with a constant temperature of 36°C and a humidity of 55% on the day of birth. Neonatal mice were fed with LPS (2 mg/kg) for 3 days, then exposed to hypoxia (99% N2) for 1 min followed hypothermia (4°C) for 10 min twice daily for 3 days. Neonatal mice were orally administered with Fusobacterium nucleatum (2×10^9 CFU) once a day at 800 mg/kg/day for 3 days.

In Vitro Experimental Design

THP-1 cells (Cell Bank of the Chinese Academy of Sciences, Shanghai, China) were grown in Dulbecco's Modified Eagle's Medium (DMEM, Gibco, Grand Island, NY, USA), with 5% fetal bovine serum (FBS, Gibco, Grand Island, NY, USA), in a humidified 5% CO_2 incubator at 37°C. HSMECs were performed transfections using Lipofectamine 2000 (Thermo Fisher Scientific, Waltham, MA, USA). LncRNA ENO1-IT1 (0.4 μg/ml, Sangon Biotech Co., Ltd. Shanghai, China), miR-22-3p (0.4 μg/ml, Sangon Biotech Co., Ltd. Shanghai, China, IRF5 (20 nmol/ml, Sangon Biotech Co., Ltd. Shanghai, China) or lncRNA ENO1-IT1 siRNAs (20 nmol/ml, Sangon Biotech Co., Ltd. Shanghai, China), miR-22-3p siRNAs (20 nmol/ml, Sangon Biotech Co., Ltd. Shanghai, China), IRF5 siRNAs (20 nmol/ml, Sangon Biotech Co., Ltd. Shanghai, China) were transfected in the serum-free and antibiotic free media. After 48 h of transfection, siRNAs (20 nmol/ml, Sangon Biotech (Shanghai) Co., Ltd.), were stimulated with LPS (200 ng/mL) for 4 h.

Quantitative Polymerase Chain Reaction (qPCR)

Total RNAs were isolated with TRIZOL (Takara, Dalian, China) and cDNA was synthesized using PrimeScipt RT Master Mix (Takara, Dalian, China). qPCR was performed with the ABI Prism 7500 sequence detection system according

to the Prime-Script™ RT detection kit. Relative levels of the sample mRNA expression were calculated and expressed as 2-DDCt. Primer sequences for RT-qPCR are available in Table I.

Western Blot

Colon tissue or cell samples were lysed with ice-cold RIPA buffer with complete protease and phosphatase inhibitors. The protein concentrations were measured using bicinchoninic acid (BCA) protein assay kit. Total proteins were separated by sodium dodecyl sulfate polyacrylamide gel electrophoresis (SDS-PAGE) and transferred onto polyvinylidene difluoride (PVDF) membranes. The membranes were incubated with primary antibodies: IRF5 (ab181553, 1:1000, Abcam, Shanghai, China), CD86 (ab239075, 1:1000, Abcam, Shanghai, China), CD208 (ab153932, 1:1000, Abcam, Shanghai, China) and β-Actin (ab6276, 1:5000, Abcam, Shanghai, China) after blocking with 5% bovine serum albumin (BSA) in TBS, followed by incubation with peroxidase-conjugated secondary antibodies (Santa Cruz Biotechnology, Santa, China). The signals were detected with the enhanced chemiluminescence (ECL) system and exposed by the Chemi-Doc XRS system with Image Labsoftware (Bio-Rad).

Enzyme-Linked Immunosorbent Assay (ELISA)

Total protein was diluted using phosphate-buffered saline (PBS), and measurement was performed according to the instructions of the manufacturer. MPO activity (A044-1-1), TNF-α (H052), IL-1β (H002), IL-17 (H014), IL-8 (H008) and IL-6 (H007) levels were measured from cell samples or tissue samples using commercial ELISA kits (Nanjing Jiancheng Institute of Biological Engineering, Nanjing, China).

Histological Examination

Colon tissues were harvested from each group and immersion fixated in 4% formaldehyde, embedded in paraffin. Heart sections (4 μm) were cut from Aneurysm tissue and stained with HE. Sections were viewed with a fluorescent microscope.

Microarray Experiments

Microarray experiments were performed at Genminix Informatics (China). Gene expression profiles were analyzed with the Human Exon 1.0 ST GeneChip (Affymetrix).

Immunofluorescent Staining

THP-1 cells were fixed with 4% paraformaldehyde for 15 min and incubated using 0.15% Triton X100 for 15 min at room temperature. H9c2 cells were incubated with IRF5 (ab181553, 1:500, Abcam) at 4˚C overnight after blocking with 5% BSA for 1 h. hASMCs were incubated with goat anti-rabbit IgG-cFL 555 antibody (1:100) for 2 h at room temperature and stained with DAPI for 15 min and washed with PBS for 15 min. The images of hASMCs obtained using a Zeiss Axioplan 2 fluorescent microscope (Carl Zeiss AG, Oberkochen, Germany).

Statistical Analysis

The data were entered into GraphPad Prism 5.01 Software and represented as mean values ± SD and a p-value <0.05 is considered statistically significant. Comparisons of data between groups were followed using Student's t-test or one-way analysis of variance (ANOVA), followed by Tukey's post hoc test. $p < 0.05$ was considered to denote a statistically significant difference.

Results

F. nucleatum Correlates with Patients with Neonatal NEC or Mice with Neonatal NEC

First, to investigate the function and active form of gut microbiota in NEC, we collected in-

Table I. Primer sequences for RT-qPCR.

	Forward	Reverse
IRF-5	5-GGAGTAGGGAGGATGTTTATTGG-3	5-AACTACTACCAAACCACCRCTCC-3
miR-22-3p	5-GCTGAGCCGCAGTAGTTCTT-3	5-GGCAGAGGGCAACAGTTCTT-3
ENO1-IT1	5-TCCAGAGAAGATGTTGGAGG-3	5-TTCTGAGTTTGGAAGTCAGG-3
U6	5-CGCTTCACGAATTTGCGTGTCAT--3	5-AACGCTTCCGAATTTGCGT-3
β-actin	5-AGAGGGAAATCGTGCGTGAC-3	5-CCATACCCAGGAAGGAAGGCT-3

testinal contents for metagenome analysis of gut microbiota composition. Metagenome analysis revealed the related changes of phylum, class and family of gut microbiota have occurred in patients with Neonatal NEC (Figure 1A). We performed real-time PCR analysis for bacterial species of patients with Neonatal NEC and the content of *F. nucleatum* in patients with Neonatal NEC was observed (Figure 1B-1C). We observed the most significant correlations between 18F-FDG maximum uptake values (SUVmax) and the abundance of *F. nucleatum* in patients with Neonatal NEC (Figure 1D). Additional Principal coordinates analysis (PCoA) plot analysis showed the hypothesis that the change of gut microbiota in patients with Neonatal NEC and *F. nucleatum* (Figure 1E). The content of *F. nucleatum* by real-time PCR in mice with Neonatal NEC was elevated (Figure 1F). Consequently, *F. nucleatum* may be the most effective pathogenic factor for Neonatal NEC.

F. nucleatum Promoted Colitis in Mice of Neonatal NEC or in Vitro Model of Neonatal NEC

To test the effects of *F. nucleatum* in mice or *in vitro* model, mice of Neonatal NEC were treated with high, middle or low dose of *F. nucleatum*. *F. nucleatum* aggravated colitis and histochemical score, increased MPO activity levels, and promoted TNF-α, IL-1β, IL-17 and IFN-gamma levels in colon tissue of mice with Neonatal NEC in time dependence (Figure 2A-2G). Similarly, *F. nucleatum* increased IL-1β, IL-8, TNF-α and

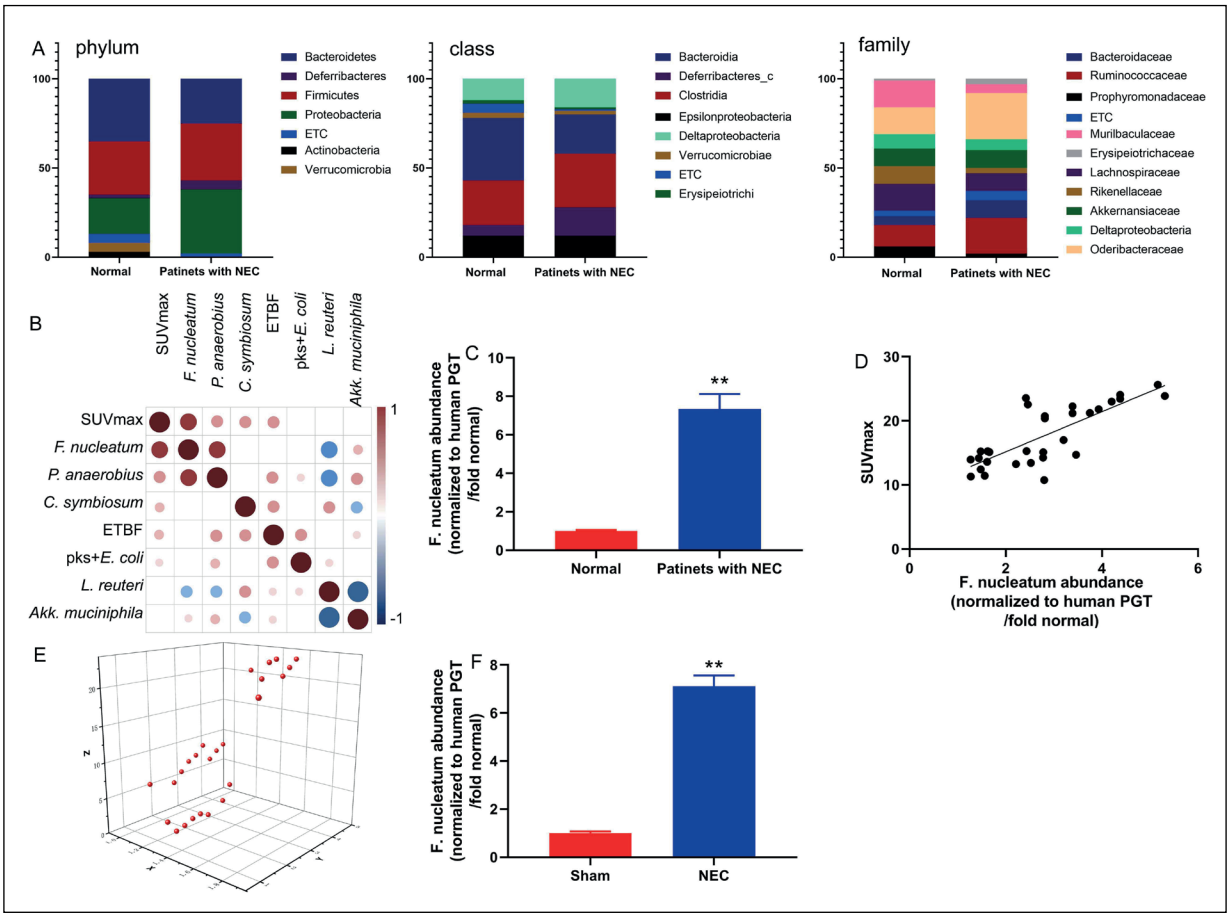

Figure 1. *F. nucleatum* correlates with patients with Neonatal NEC or mice with Neonatal NEC. Compositional analysis of mouse gut microbiota using 16 S rRNA full sequencing (**A**), Spearman's correlation between taxa enrichment and 18F-FDG uptake in patients with Neonatal NEC by real-time PCR (**B**), the content of *F. nucleatum* by real-time PCR (**C**), the most significant correlations between 18F-FDG maximum uptake values (SUVmax) and the abundance of *F. nucleatum* in patients with Neonatal NEC (**D**), Principle coordinates analysis (PCoA) plot with the weighted Unifrac distance matrix (**E**) in patients with Neonatal NEC; the content of *F. nucleatum* by real-time PCR in mice with Neonatal NEC (**F**). Normal, normal group; patients with Neonatal NEC group; sham, sham control group; NEC, mice with NEC group. $^{**}p<0.01$ compared with normal group or mice with NEC group.

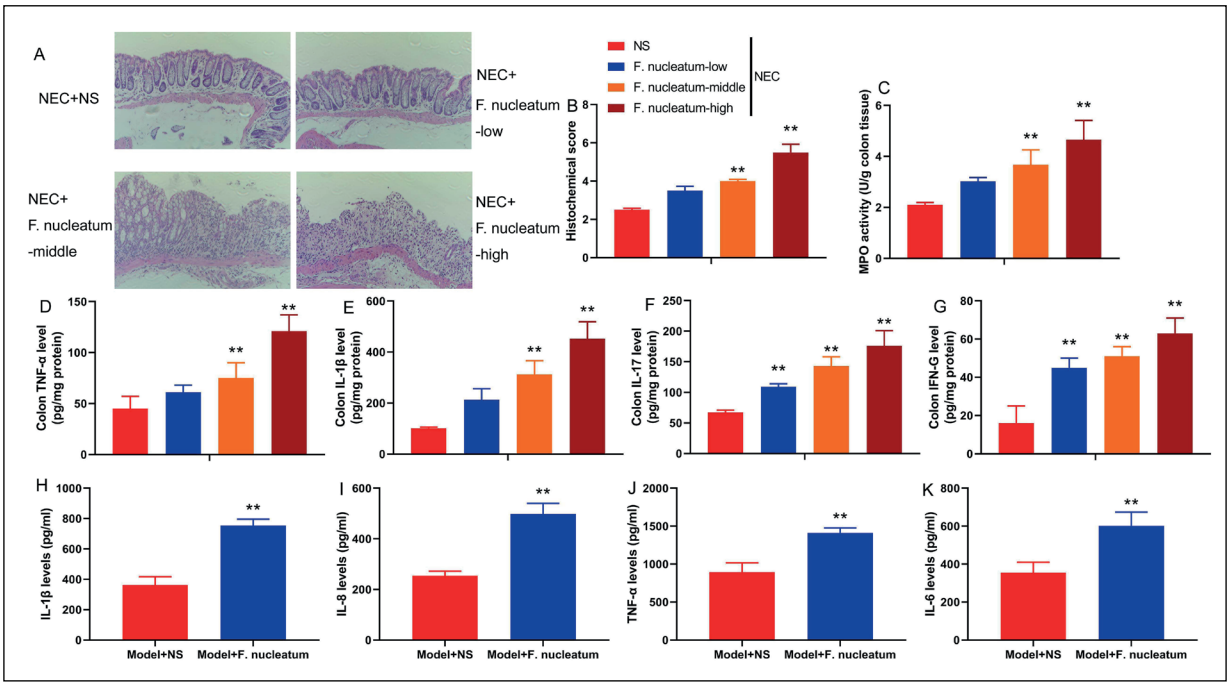

Figure 2. *F. nucleatum* promoted colitis in mice of Neonatal NEC or *in vitro* model of Neonatal NEC Colitis tissue (100X, **A**), histochemical score (**B**), MPO activity levels (c), TNF-α (**D**), IL-1β (**E**), IL-17 (**F**) and IFN-gamma (**G**) levels in colon tissue of mice with Neonatal NEC; IL-1β (**H**), IL-8 (**I**), TNF-α (**J**) and IL-6 (**K**) levels *in vitro* model. NEC, mice with Neonatal NEC; NS, normal saline; *F. nucleatum*-low, mice with Neonatal NEC by low dose of *F. nucleatum*; *F. nucleatum*-middle, mice with Neonatal NEC by middle dose of *F. nucleatum*; *F. nucleatum*-middle, mice with Neonatal NEC by high dose of *F. nucleatum*; Model+NS, *in vitro* model by normal saline; Model+ *F. nucleatum*, *in vitro* model by *F. nucleatum*. $^{**}p<0.01$ compared with mice with Neonatal NEC or *in vitro* model by normal saline.

IL-6 levels *in vitro* model (Figure 2H-2K). In general, data suggest that *F. nucleatum* promotes colitis in Neonatal NEC.

F. nucleatum Activates Inflammation Via a Selective Increase of LncRNA ENO1-IT1

To investigate the mechanism of *F. nucleatum* in Neonatal NEC, we analyzed the target gene in Neonatal NEC. Microarray analysis showed that lncRNA ENO1-IT1 may be a target gene of *F. nucleatum in vitro* model of NEC (Figure 3A-3B). LncRNA ENO1-IT1 expression was induced in mice treated with high, middle or low dose of *F. nucleatum* (Figure 3C). *F. nucleatum* enhanced lncRNA ENO1-IT1 expression *in vitro* model, other microbiotas not affected the expression of lncRNA ENO1-IT1 (Figure 3D-3E). Next, we used si-ENO1-IT1 mimics to reduce IL-1β, IL-8, TNF-α and IL-6 levels *in vitro* model by treated with *F. nucleatum* (Figure 3F-3I). Next, we analyzed the function of lncRNA ENO1-IT1 in neonatal NEC. There were increases of lncRNA ENO1-IT1 expression in lncRNA ENO1-IT1 group and the inhibition of lncRNA ENO1-IT1 expression was observed in si-lncRNA ENO1-IT1 group (Figure 4A). Over-expression of lncRNA ENO1-IT1 increased IL-1β, IL-8, TNF-α and IL-6 levels *in vitro* model inducted with LPS (Figure 4B-4D). Down-regulation of lncRNA ENO1-IT1 reduced IL-1β, IL-8, TNF-α and IL-6 levels *in vitro* model inducted with LPS (Figure 4F-4I). In conclusion, these finding indicate that *F. nucleatum* activates inflammation *via* a selective increase of lncRNA ENO1-IT1.

LncRNA ENO1-IT1 the Regulation Network Associated with MiR-22-3p

The study further investigated the mechanism of *F. nucleatum* in Neonatal NEC via lncRNA ENO1-IT1 using microarray analysis. MiR-22-3p was screened and may be a target spot for LncRNA ENO1-IT1 in the effects of *F. nucleatum* on inflammation in Neonatal NEC (Figure 5A). Subcellular analysis demonstrated that miR-22-3p was located in the cytoplasmic portion, suggesting potential post-transcriptional regulation (Figure 5B). The wild-type (WT) and corre-

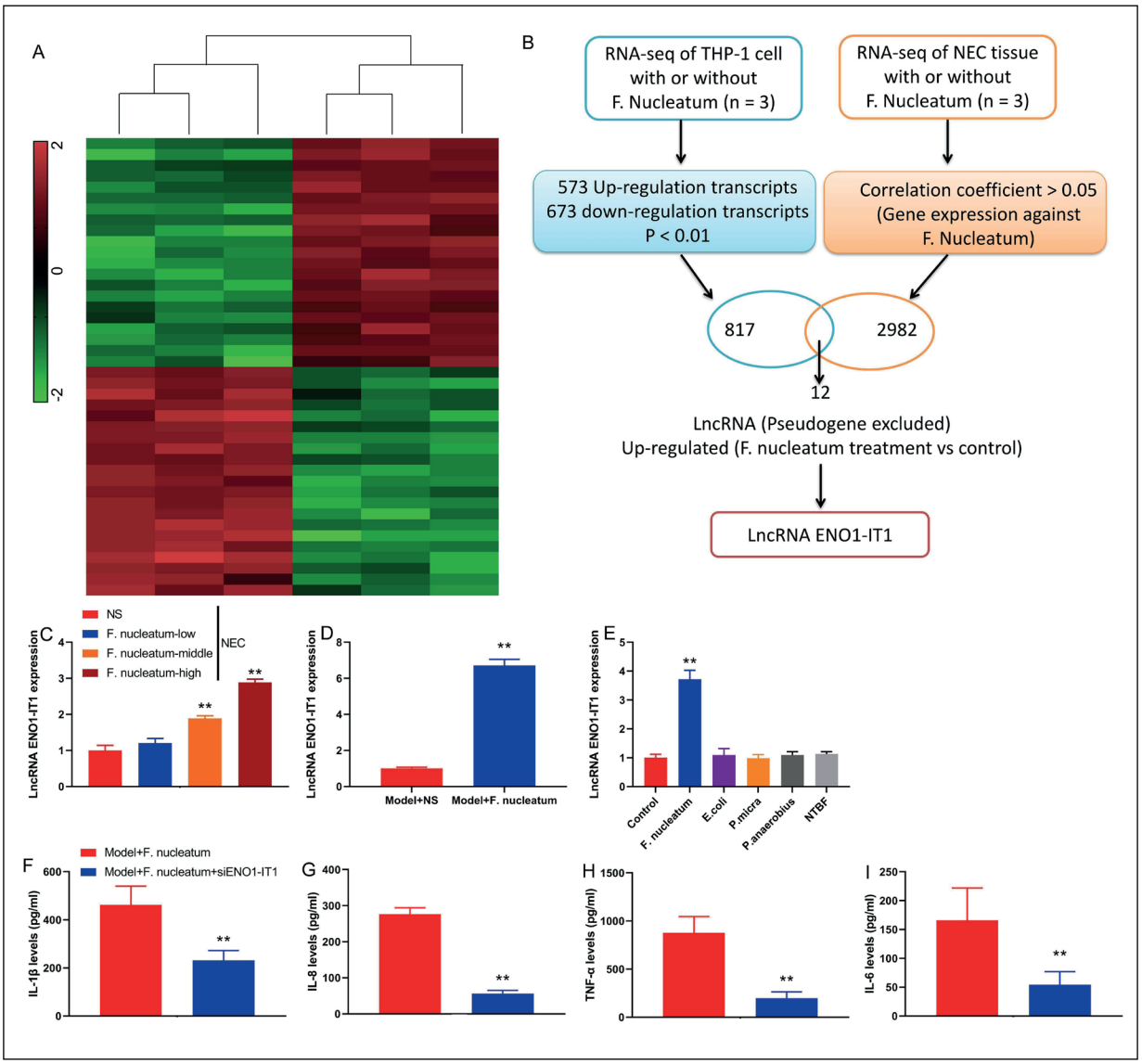

Figure 3. *F. nucleatum* activates inflammation via a selective increase of lncRNA ENO1-IT1. Heat map (**A**) and analysis result (**B**); lncRNA ENO1-IT1 expression in mice with Neonatal NEC by *F. nucleatum* (**C**); lncRNA ENO1-IT1 expression *in vitro* with Neonatal NEC by *F. nucleatum* (**D** and **E**); IL-1β (**F**), IL-8 (**G**), TNF-α (**H**) and IL-6 (**I**) levels *in vitro* model. NEC, mice with Neonatal NEC; NS, normal saline; *F. nucleatum*-low, mice with Neonatal NEC by low dose of *F. nucleatum*; *F. nucleatum*-middle, mice with Neonatal NEC by middle dose of *F. nucleatum*; *F. nucleatum*-middle, mice with Neonatal NEC by high dose of *F. nucleatum*; Model+NS, *in vitro* model by normal saline; Model+ *F. nucleatum*, *in vitro* model by *F. nucleatum*. ***p*<0.01 compared with mice with Neonatal NEC or *in vitro* model by normal saline.

sponding mutant (Mut) were constructed targeting miR-22-3p, and a Luciferase reporter assay illustrated that lncRNA ENO1-IT1 WT closely correlated with miR-22-3p (Figure 5C). *F. nucleatum* reduced miR-22-3p expression in mice with neonatal NEC and *in vitro* model of neonatal NEC (Figure 5D-5E). The inhibition of lncRNA ENO1-IT1 increased *in vitro* model of neonatal NEC by *F. nucleatum* (Figure 5F). RNA-FISH demonstrated the distribution of lncRNA ENO1-IT1 and miR-22-3p in cytoplasm and nuclear material (Figure 5G). Over-expression of lncRNA ENO1-IT1 inhibited the expression of miR-22-3p and down-regulation of lncRNA ENO1-IT1 increased miR-22-3p *in vitro* model inducted with LPS (Figure 5H-5I).

Next, miR-22-3p plasmid increased the expression of miR-22-3p, and increased IL-1β, IL-8,

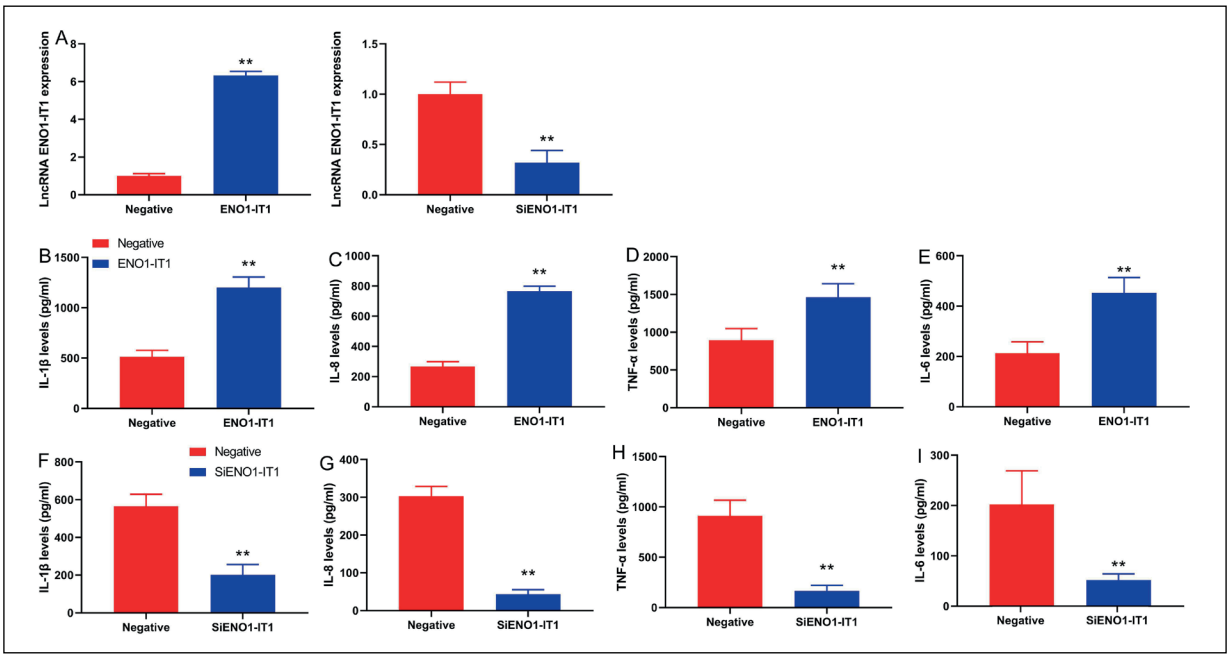

Figure 4. F. LncRNA ENO1-IT1 activates inflammation *in vitro* model of *F. nucleatum*. LncRNA ENO1-IT1 expression (**A**); IL-1β (**B**), IL-8 (**C**), TNF-α (**D**) and IL-6 (**E**) levels *in vitro* model by over-expression of lncRNA ENO1-IT1; IL-1β (**F**), IL-8 (**G**), TNF-α (**H**) and IL-6 (**I**) levels *in vitro* model by down-regulation of lncRNA ENO1-IT1. Negative, *in vitro* model by negative group; ENO1-IT1, *in vitro* model by over-expression of ENO1-IT1 group; Si-ENO1-IT1, *in vitro* model by over-expression of ENO1-IT1 group. $^{**}p<0.01$ compared with mice with Neonatal NEC or *in vitro* model by normal saline.

TNF-α and IL-6 levels *in vitro* model of neonatal NEC by *F. nucleatum* (Figure 6A-6E). MiR-22-3p plasmid or si-miR-22-3p mimics increased miR-22-3p expression or reduced miR-22-3p expression *in vitro* model inducted with LPS (Figure 6F-6G). Over-expression of miR-22-3p reduced IL-1β, IL-8, TNF-α and IL-6 levels *in vitro* model inducted with LPS (Figure 6H-6K). Down-regulation of miR-22-3p induced IL-1β, IL-8, TNF-α and IL-6 levels *in vitro* model inducted with LPS (Figure 6L-6O). These data suggest that miR-22-3p plays an essential role in *F. nucleatum* mediated-inflammation of Neonatal NEC.

MiR-22-3p Associated with IRF5 Expression in F. nucleatum in Neonatal NEC Via LncRNA ENO1-IT1

The study further investigated the mechanism of *F. nucleatum* in Neonatal NEC via lncRNA ENO1-IT1 by miR-22-3p using microarray analysis. IRF5 was screened and may be a target spot for LncRNA ENO1-IT1/miR-22-3p in the effects of *F. nucleatum* on inflammation in Neonatal NEC (Figure 7A). Over-expression of lncRNA ENO1-IT1 increased the mRNA expression of IRF5, over-expression of miR-22-3p suppressed IRF5 mRNA expression, and over-expression of miR-22-3p reduced the effects of lncRNA ENO1-IT1 on the increases of IRF5 mRNA expression *in vitro* model (Figure 7B). Down-regulation of lncRNA ENO1-IT1 decreased the mRNA expression of IRF5, down-regulation of miR-22-3p induced IRF5 mRNA expression, and down-regulation of miR-22-3p reversed the effects of si-lncRNA ENO1-IT1 on the increases of IRF5 mRNA expression *in vitro* model (Figure 7C). The wild-type (WT) and corresponding mutant (Mut) were constructed targeting miR-22-3p, and a luciferase reporter assay illustrated that IRF5 WT closely correlated with miR-22-3p (Figure 7D). Over-expression of miR-22-3p reduced IRF5 expression *in vitro* model (Figure 7E).

Next, *F. nucleatum* induced IRF5 protein expression in mice model of Neonatal NEC or *in vitro* model of Neonatal NEC (Figure 8A-8D). Si-lncRNA ENO1-IT1 suppressed IRF5 protein expression *in vitro* model of Neonatal NEC by *F. nucleatum* (Figure 8E-8F). Over-expression of ENO1-IT1 induced IRF5 protein expression, and down-regulation of ENO1-IT1 suppressed IRF5 protein expression *in vitro* model inducted with LPS (Figure 8G-8H). Down-regulation of ENO1-IT1 suppressed IRF5 protein expression *in vitro* model inducted with LPS (Figure 8I-8J). Fur-

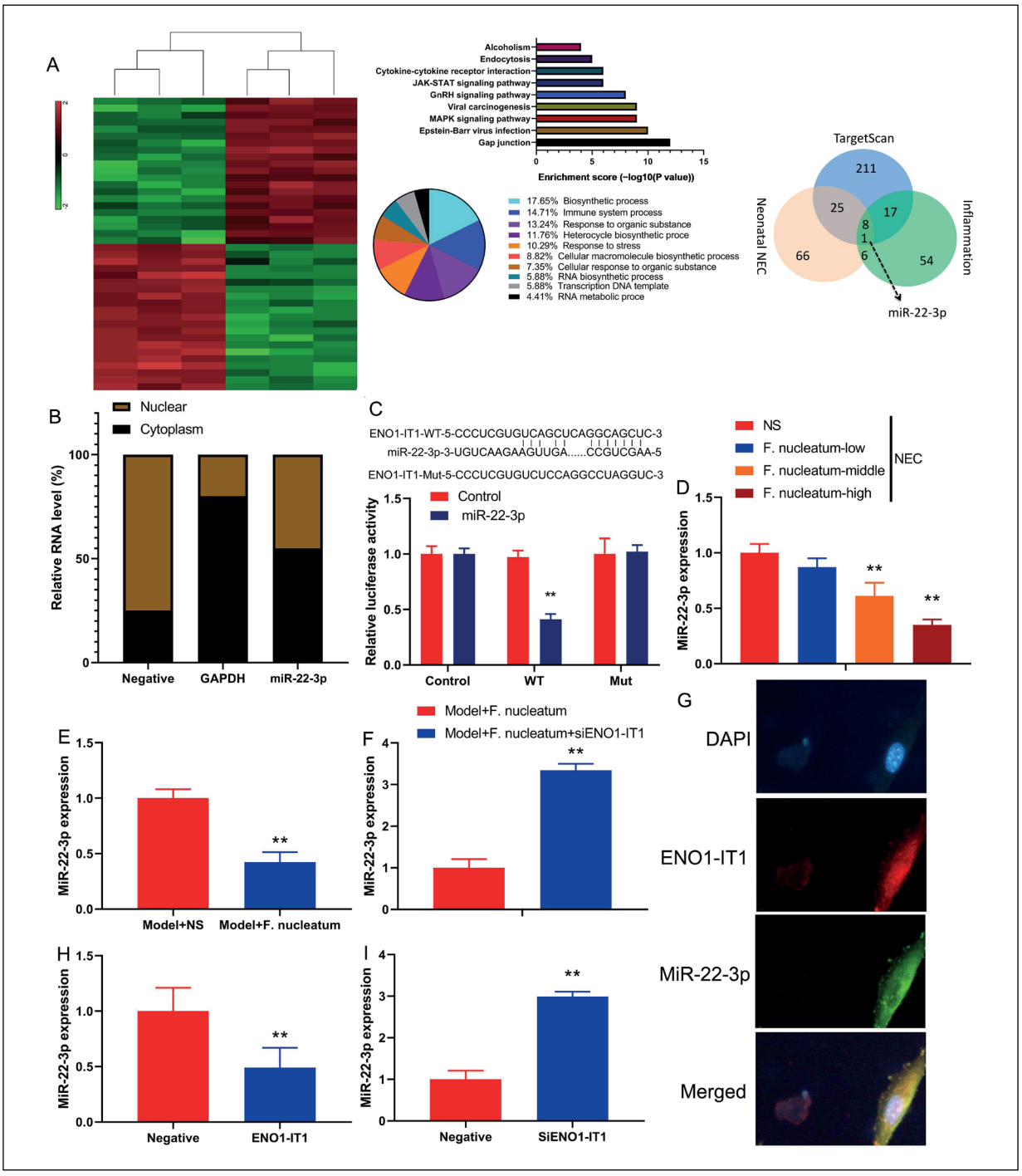

Figure 5. LncRNA ENO1-IT1 the regulation network associated with miR-22-3p. Heat map and analysis result (**A**); relative mRNA expression (**B**); relative luciferase activity (**C**); miR-22-3p mRNA expression in mice with Neonatal NEC by *F. nucleatum* (**D**); miR-22-3p mRNA expression (**E**) *in vitro* with Neonatal NEC by *F. nucleatum*; miR-22-3p mRNA expression (**F**) *in vitro* with Neonatal NEC by *F. nucleatum* and down-regulation of ENO1-IT1; RNA-FISH demonstrated the distribution of lncRNA ENO1-IT1 and miR-22-3p **(G)**; miR-22-3p mRNA expression (**H**) *in vitro* model by over-expression of lncRNA ENO1-IT1; miR-22-3p mRNA expression (**I**) *in vitro* model by down-regulation of lncRNA ENO1-IT1; NEC, mice with Neonatal NEC; NS, normal saline; *F. nucleatum*-low, mice with Neonatal NEC by low dose of *F. nucleatum*; *F. nucleatum*-middle, mice with Neonatal NEC by middle dose of *F. nucleatum*; *F. nucleatum*-middle, mice with Neonatal NEC by high dose of *F. nucleatum*; Model+NS, *in vitro* model by normal saline; Model+ *F. nucleatum*, *in vitro* model by *F. nucleatum*; Negative, *in vitro* model by negative group; ENO1-IT1, *in vitro* model by over-expression of ENO1-IT1 group; Si-ENO1-IT1, *in vitro* model by down-regulation of ENO1-IT1 group. ***p*<0.01 compared with mice with Neonatal NEC or *in vitro* model by normal saline.

thermore, miR-22-3p over-expression suppressed IRF5 protein expression *in vitro* model of Neonatal NEC by *F. nucleatum* and over-expression of ENO1-IT1 (Figure 8K-8L). Over-expression of miR-22-3p induced IRF5 protein expression, and down-regulation of miR-22-3p suppressed IRF5 protein expression *in vitro* model inducted with LPS (Figure 8M-8P).

The Inhibition IRF5 Reduced the Effects of F. nucleatum on Inflammation In Vitro Model of Neonatal NEC Via CD206 and CD86 Expression

In order to investigate the role and mechanism of IRF5 in the effects of *F. nucleatum* on inflammation *in vitro* model of Neonatal NEC. Si-IRF5 suppressed IRF5 protein expression *in vitro* model by over-expression of lncRNA ENO1-IT1 (Figure 9A). IRF5 plasmid induced IRF5 protein expression, si-IRF5 suppressed IRF5 protein expression *in vitro* model inducted with LPS (Figure 9B-9C). Over-expression of IRF5 increased IL-1β, IL-8, TNF-α and IL-6 levels *in vitro* model inducted with LPS (Figure 9D-9G). Down-regulation of IRF5 reduced IL-1β, IL-8, TNF-α and IL-6 levels *in vitro* model inducted with LPS (Figure 9H-9K). Then, we found that Si-IRF5 suppressed CD68 protein expression and induced CD206 protein expression *in vitro* model by over-expression of lncRNA ENO1-IT1 (Figure

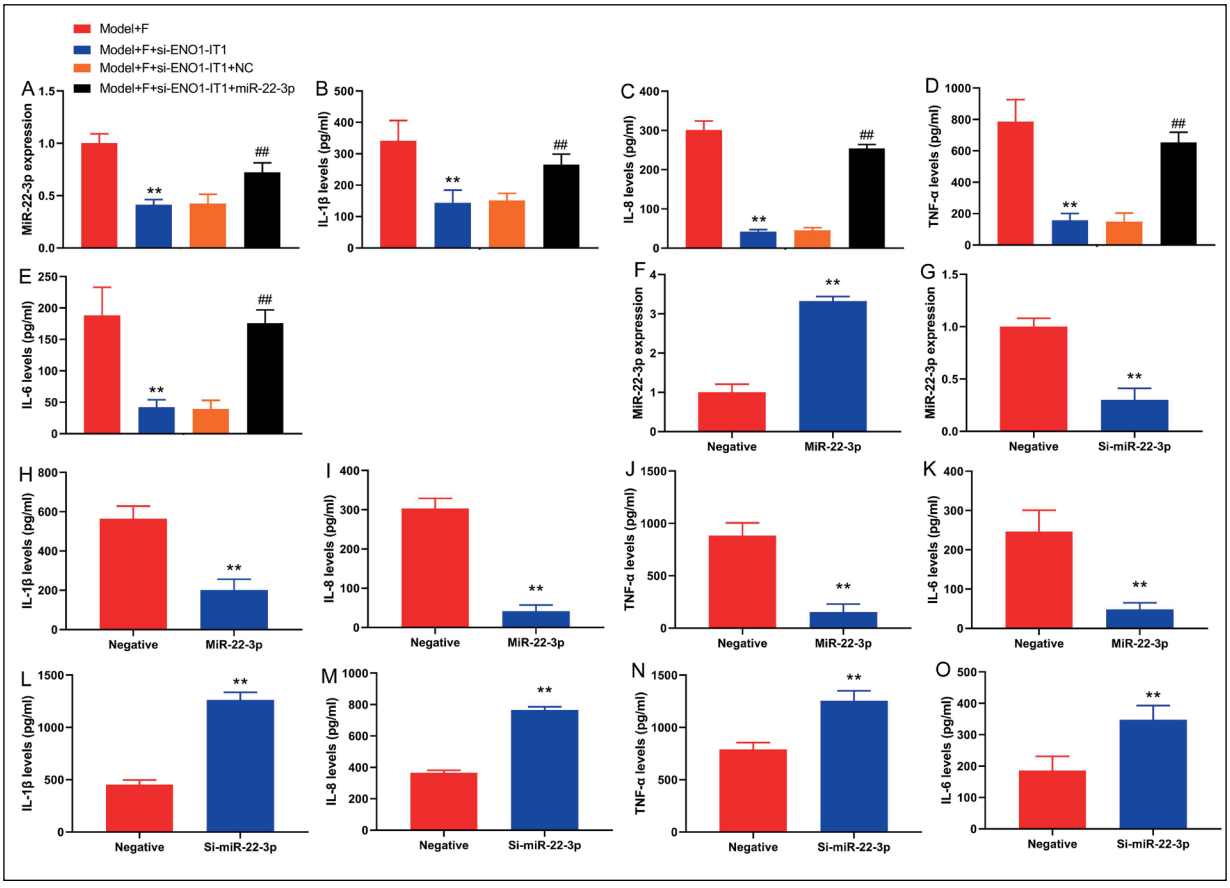

Figure 6. MiR-22-3p reduced inflammation *in vitro* model of *F. nucleatum*. MiR-22-3p expression (**A**), IL-1β (**B**), IL-8 (**C**), TNF-α (**D**) and IL-6 (**E**) levels *in vitro* model by *F. nucleatum*, down-regulation of lncRNA ENO1-IT1 and over-expression of miR-22-3p; miR-22-3p expression (**F** and **G**) *in vitro* model; IL-1β (**H**), IL-8 (**I**), TNF-α (**J**) and IL-6 (**K**) levels *in vitro* model by over-expression of ENO1-IT1 group; IL-1β (**L**), IL-8 (**M**), TNF-α (**N**) and IL-6 (**O**) levels *in vitro* model by down-regulation of ENO1-IT1 group. Model+F, *in vitro* model with Neonatal NEC by *F. nucleatum*; Model+F+si-ENO1-IT1, *in vitro* with Neonatal NEC by *F. nucleatum* and down-regulation of ENO1-IT1; Model+F+si-ENO1-IT1+NC, *in vitro* with Neonatal NEC by *F. nucleatum*, down-regulation of ENO1-IT1 and negative mimics; Model+F+si-ENO1-IT1+ miR-22-3p, *in vitro* with Neonatal NEC by *F. nucleatum*, down-regulation of ENO1-IT1 and over-expression of miR-22-3p; Negative, *in vitro* model by negative group; miR-22-3p, *in vitro* model by over-expression of miR-22-3p group; Si- miR-22-3p, *in vitro* model by down-regulation of miR-22-3p group. $^{**}p<0.01$ compared with mice with Neonatal NEC or *in vitro* model by normal saline.

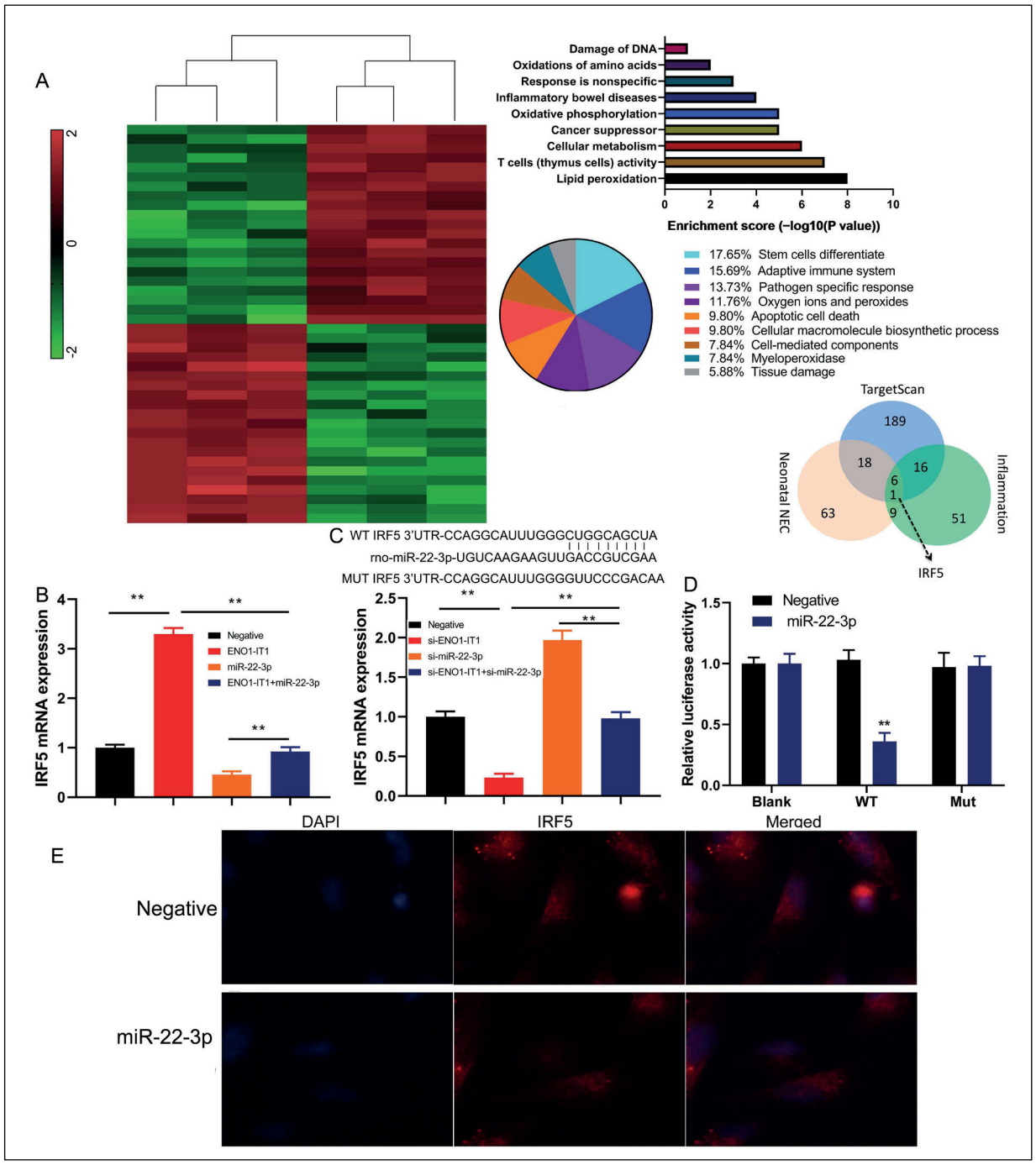

Figure 7. MiR-22-3p associated with IRF5 expression in *F. nucleatum* in Neonatal NEC *via* lncRNA ENO1-IT1. Heat map and analysis result (**A**), IRF5 mRNA expression (**B** and **C**), relative luciferase activity (**D**), IRF5 expression (400X, **F**, **E**). Negative, negative group; miR-22-3p, over-expression of miR-22-3p group. $^{**}p<0.01$ is considered statistically significant.

9L-9M). Over-expression of IRF5 induced CD68 protein expression and suppressed CD206 protein expression *in vitro* model inducted with LPS (Figure 9N-9O). Down-regulation of IRF5 suppressed CD68 protein expression and induced CD206 protein expression *in vitro* model inducted with LPS (Figure 9P-9Q). therefore, IRF5 might play an important role in the effects of *F. nucleatum* on inflammation *in vitro* model of Neonatal NEC via CD206 and CD86 expression.

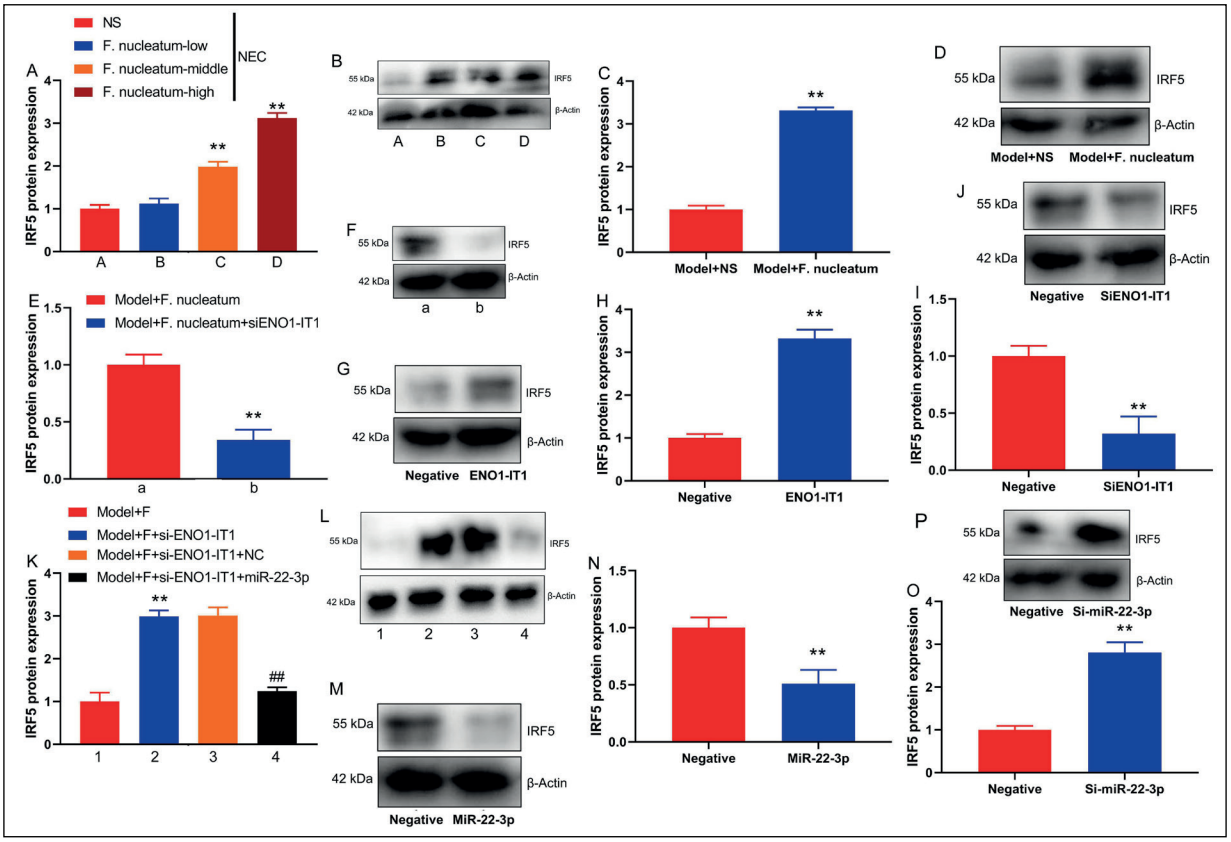

Figure 8. IRF5 promoted inflammation *in vitro* model of *F. nucleatum*. IRF5 protein expression in mice with *F. nucleatum* (**A** and B), IRF5 protein expression *in vitro* with *F. nucleatum* (**C** and **D**), IRF5 protein expression *in vitro* with *F. nucleatum* and si-lncRNA ENO1-IT1 (**E** and **F**), IRF5 protein expression *in vitro* by over-expression of lncRNA ENO1-IT1 (**G** and **H**), IRF5 protein expression *in vitro* by down-regulation of lncRNA ENO1-IT1 (**I** and **J**), IRF5 protein expression *in vitro* with *F. nucleatum*, si-lncRNA ENO1-IT1 and over-expression of miR-22-3p (**K** and **L**), IRF5 protein expression *in vitro* by over-expression of miR-22-3p (**M** and **N**), IRF5 protein expression *in vitro* by down-regulation of miR-22-3p (**O** and **P**), Model+F, *in vitro* model with Neonatal NEC by *F. nucleatum*; Model+F+ENO1-IT1, *in vitro* with Neonatal NEC by *F. nucleatum* and over-regulation of ENO1-IT1; Model+F+ENO1-IT1+NC, *in vitro* with Neonatal NEC by *F. nucleatum*, over-regulation of ENO1-IT1 and negative mimics; Model+F+ENO1-IT1+siIRF5, *in vitro* with Neonatal NEC by *F. nucleatum*, over-regulation of ENO1-IT1 and down-regulation of IRF5; Negative, *in vitro* model by negative group; IRF5, *in vitro* model by over-expression of IRF5 group; Si- IRF5, *in vitro* model by down-regulation of IRF5 group. $^{**}p<0.01$ compared with mice with Neonatal NEC or *in vitro* model by normal saline.

Discussion

NEC is a common disease in newborns, characterized by high incidence and high mortality[15]. However, the pathogenic factors of NEC have not yet been fully clarified, which is considered to be associated with neonatal congenital malformations, hypoxia and asphyxia[16]. Some scholars believe that bacterial infection and abnormal red blood cells may be one of the main causes of NEC. NEC is characterized by rapid onset and rapid progress[17]. It is a relatively severe digestive system disease in the newborn period, which can cause death in lethal cases[18]. Therefore, early diagnosis and timely treatment of children are of great significance to the prognosis. The present study demonstrated that the content of *F. nucleatum* was increased in patients with Neonatal NEC. Liu et al[19] showed that *F. nucleatum* aggravates colitis via M1 Macrophage Polarization. The above results indicated that *F. nucleatum* may be the most effective pathogenic factor for Neonatal NEC.

In recent years, many reports have shown that the imbalance of gut microbiota is an important and basic cause of NEC[20]. Therefore, the key to attenuating NEC damage is prevention. Among them, the application of probiotics is currently the research focus[21]. Our data showed that *F. nucleatum* promoted colitis in mice of Neonatal

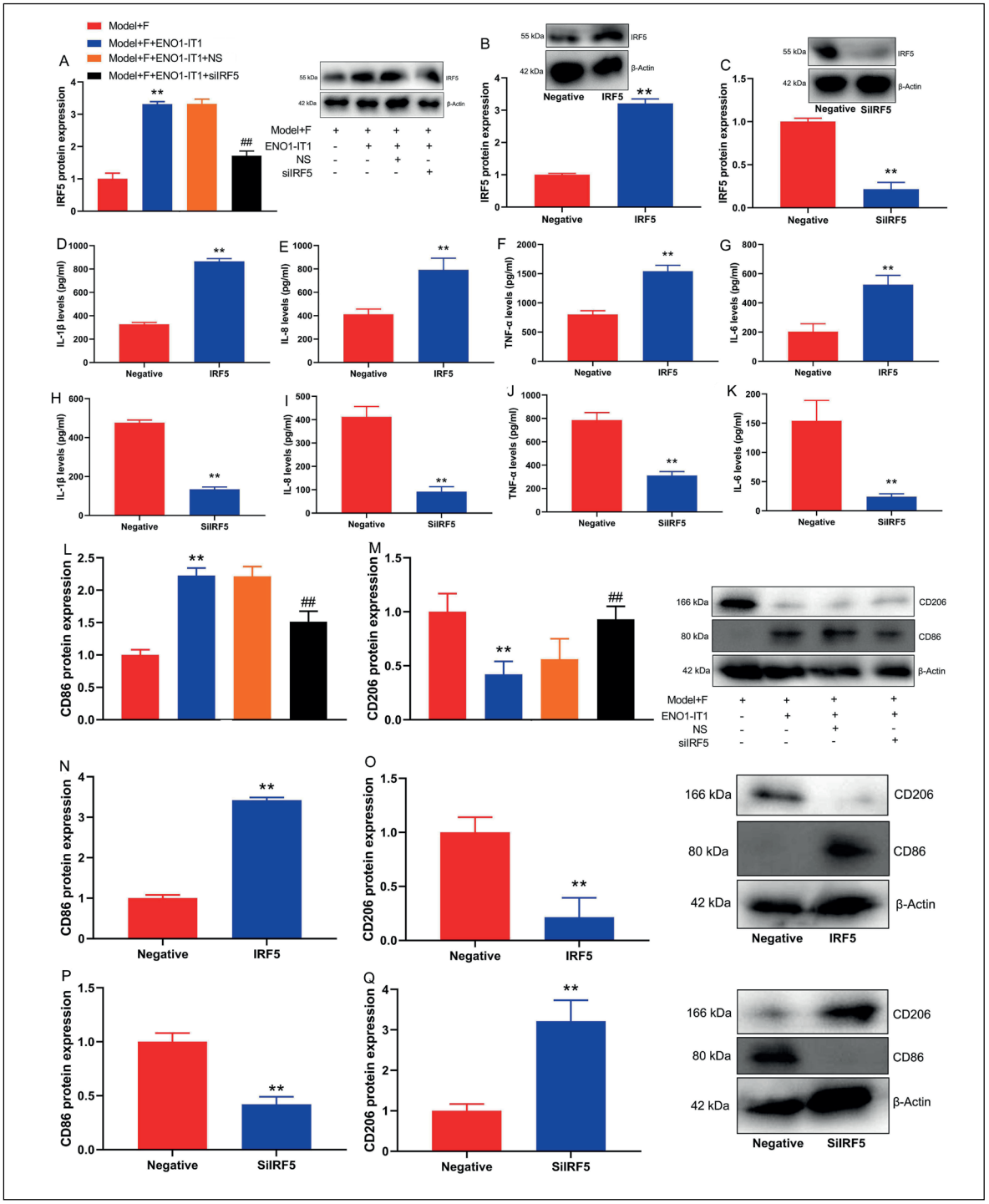

Figure 9. The inhibition IRF5 reduced the effects of *F. nucleatum* on inflammation *in vitro* model of Neonatal NEC via CD206 and CD86 expression. IRF5 protein expression (**A**, **B** and **C**); IL-1β (**D**), IL-8 (**E**), TNF-α (**F**) and IL-6 (**G**) levels *in vitro* model by over-expression of IRF5; IL-1β (**H**), IL-8 (**I**), TNF-α (**J**) and IL-6 **(K)** levels *in vitro* model by down-regulation of IRF5; CD206 and CD86 protein expressions (**L** and **M**) *in vitro* model; CD206 and CD86 protein expressions (**N** and **O**) *in vitro* model by over-expression of IRF5; CD206 and CD86 protein expressions (**P** and **Q**) *in vitro* model by down-regulation of IRF5. Model+F, *in vitro* model with Neonatal NEC by *F. nucleatum*; Model+F+ENO1-IT1, *in vitro* with Neonatal NEC by *F. nucleatum* and over-regulation of ENO1-IT1; Model+F+ENO1-IT1+NC, *in vitro* with Neonatal NEC by *F. nucleatum*, over-regulation of ENO1-IT1 and negative mimics; Model+F+ENO1-IT1+siIRF5, *in vitro* with Neonatal NEC by *F. nucleatum*, over-regulation of ENO1-IT1 and down-regulation of IRF5; Negative, *in vitro* model by negative group; IRF5, *in vitro* model by over-expression of IRF5 group; Si- IRF5, *in vitro* model by down-regulation of IRF5 group. **$p<0.01$ compared with mice with Neonatal NEC or *in vitro* model by normal saline.

NEC or *in vitro* model of Neonatal NEC. Liu et al[22] reported that *F. nucleatum* exacerbates colitis by inducing aberrant inflammation. Our results demonstrated that *F. nucleatum* was an important pro-inflammatory factor in model of Neonatal NEC.

LncRNAs play different roles in different biological processes and lncRNAs function as a key regulator in immunity and gene regulation[23]. In-depth research to understand the function of lncRNA and its immune regulation in UC, as well as the specificity of lncRNA can provide novel approaches for targeted therapy and diagnosis of UC[24,25]. Our results supported that *F. nucleatum* activates inflammation via a selective increase of lncRNA ENO1-IT1. Hong et al supported *F. nucleatum* promoted oncogenesis in colorectal cancer by lncRNA ENO1-IT1[26]. Similarly, *F. nucleatum* promoted inflammation by targeting lncRNA ENO1-IT1 in Neonatal NEC.

Macrophages are an important type of immune cells in the body, which play a vital role in pro-inflammatory, anti-inflammatory and tissue repair processes[20]. Plasticity is an important feature of macrophages, that is, macrophages can adjust their phenotype and function according to changes in the microenvironment, which is also the origin of macrophages polarization[27,28]. The result showed that miR-22-3p plays an essential role in *F. nucleatum* mediated-inflammation of Neonatal NEC. Liu et al[29] confirmed that circ-AMOTL1/ENO1/miR-22-3p implicated in the tumorigenesis of oral squamous cell carcinoma.

IRF5 plays an important role in IFN transcription regulation, pathogen immune response, cytokine signal transduction and immune regulation[30]. IRF5 can regulate the production of IFN-α, induce the expression of various inflammatory factors (including IL-6, IL-12, IL-23, TNF, etc.), playing diverse roles in the body[31-33]. Our study suggested that miR-22-3p is associated with IRF5 expression in *F. nucleatum* in Neonatal NEC via lncRNA ENO1-IT1. Fang et al[34] demonstrated that miR-22-3p reduced the progression of spinal cord I/R injury via IRF5. These results showed that IRF5 might be an important therapeutic target for the effects of *F. nucleatum* in *F. nucleatum* through lncRNA ENO1-IT1/miR-22-3p.

CD68 is a protein component mainly expressed on the surface of macrophages and a few monocytes[35]. Functionally, CD68 reflects the presence and chemotactic aggregation of macrophages, and is correlated with inflammation[36]. CD206 is a specific marker of M2 macrophages and an important indicator of NEC treatment[37]. Consistently, we demonstrated that the inhibition IRF5 reduced the effects of *F. nucleatum* on inflammation *in vitro* model of Neonatal NEC via CD206 and CD86 expression. Xie et al[38] suggest that *IRF5* is involved in the *M1* polarization of macrophages. These data showed that IRF5 regulated CD206 and CD86 expression in model of Neonatal NEC by F. nucleate via lncRNA ENO1-IT1/miR-22-3p.

Conclusions

Collectively, the present study confirmed that *F. nucleatum* promoted inflammation of Neonatal NEC by LncRNA ENO1-IT1/miR-22-3p/IRF5 pathway. LncRNA ENO1-IT1 may be important targets for *F. nucleatum* in NEC-inflammation, and significant in treating patients with Neonatal NEC with elevated *F. nucleatum*. Furthermore, the present results provide a theoretical basis for gut microbiota as a preventive and therapeutic agent for Neonatal NEC in the future. LncRNA ENO1-IT1 might provide a new insight into Neonatal NEC.

Conflict of Interest

The Authors declare that they have no conflict of interests.

Acknowledgements

This work was supported by the Fuzhou Key Clinical Specialty Construction Project (20191-2007) and the Fuzhou Science and Technology Plan Project (2019-SZ-54, 2020-S-wq23, 2020-WS-62, 2020-WS-75) and Fuzhou Key Clinical Specialty Construction Project (201912007).

References

1) Cohen M, Steffen E, Axelrod R, Patel SN, Toczylowski K, Perdon C, Brown D, Kaliappan S, Myers M. Availability of Donor Human Milk Decreases the Incidence of Necrotizing Enterocolitis in VLBW Infants. Adv Neonatal Care. 2020 Dec 10. doi: 10.1097/ANC.0000000000000804. Epub ahead of print.
2) Gałązka P, M Chrzanowska, J Styczyński. Clinical Spectrum and Outcomes of Neonatal Necrotizing Enterocolitis. In Vivo 2021; 35: 585-591.
3) Good M, T Chu, P Shaw, L Mcclain, A Chamberlain, C Castro, JM Rimer, B Mihi, Q Gong, LS Nolan, K Cooksey, L Linneman, P Agrawal, DN Fine-

gold, D Peters. Global hypermethylation of intestinal epithelial cells is a hallmark feature of neonatal surgical necrotizing enterocolitis. Clin Epigenetics 2020; 12: 190.

4) Granger CL, Embleton ND, Palmer JM, Lamb CA, Berrington JE, Stewart CJ. Maternal breastmilk, infant gut microbiome and the impact on preterm infant health. Acta Paediatr 2021; 110: 450-457.
5) Bering SB. Human Milk Oligosaccharides to Prevent Gut Dysfunction and Necrotizing Enterocolitis in Preterm Neonates. Nutrients 2018; 10: 1461.
6) Hackam D, Caplan M. Necrotizing enterocolitis: Pathophysiology from a historical context. Semin Pediatr Surg 2018; 27: 11-18.
7) Willers M, Ulas T, Völlger L, Vogl T, Heinemann AS, Pirr S, Pagel J, Fehlhaber B, Halle O, Schöning J, Schreek S, Löber U, Essex M, Hombach P, Graspeuntner S, Basic M, Bleich A, Cloppenborg-Schmidt K, Künzel S, Jonigk D, Rupp J, Hansen G, Förster R, Baines JF, Härtel C, Schultze JL, Forslund SK, Roth J, Viemann D. S100A8 and S100A9 Are Important for Postnatal Development of Gut Microbiota and Immune System in Mice and Infants. Gastroenterology 2020; 159: 2130-2145.e5.
8) Chen H, L Zeng, W Zheng, X Li, B Lin. Increased Expression of microRNA-141-3p Improves Necrotizing Enterocolitis of Neonates Through Targeting MNX1. Front Pediatr 2020; 8: 385.
9) Liu H, YB Wang. Systematic large-scale meta-analysis identifies miRNA-429/200a/b and miRNA-141/200c clusters as biomarkers for necrotizing enterocolitis in newborn. Biosci Rep 2019; 39.
10) Walker SJ, CD Langefeld, K Zimmerman, MZ Schwartz, A Krigsman. A molecular biomarker for prediction of clinical outcome in children with ASD, constipation, and intestinal inflammation. Sci Rep 2019; 9: 5987.
11) Xu Y, Y Liu, H Xie, Y Zhou, X Yan, W Chen, X Wang, Z Yu, F Wang, X Chen, J Wang, S Han. Profile analysis reveals endogenous RNAs regulate necrotizing enterocolitis progression. Biomed Pharmacother 2020; 125: 109975.
12) Principe M, S Borgoni, M Cascione, MS Chattaragada, S Ferri-Borgogno, M Capello, S Bulfamante, J Chapelle, F Di Modugno, P Defilippi, P Nisticò, P Cappello, C Riganti, S Leporatti, F Novelli. Alpha-enolase (ENO1) controls alpha v/beta 3 integrin expression and regulates pancreatic cancer adhesion, invasion, and metastasis. J Hematol Oncol 2017; 10: 16.
13) Cappello P, M Principe, S Bulfamante, F Novelli. Alpha-Enolase (ENO1), a potential target in novel immunotherapies. Front Biosci (Landmark Ed) 2017; 22: 944-959.
14) Zhou J, S Zhang, Z Chen, Z He, Y Xu, Z Li. CircRNA-ENO1 promoted glycolysis and tumor progression in lung adenocarcinoma through upregulating its host gene ENO1. Cell Death Dis 2019; 10: 885.
15) Karila K, Koivusalo A. The Outcome of Blood Transfusions in Conservative and Surgical Necrotizing Enterocolitis and Spontaneous Intestinal Perforation. Eur J Pediatr Surg. 2020 Dec 30. doi: 10.1055/s-0040-1721769. Epub ahead of print.
16) Lure AC, Du X, Black EW, Irons R, Lemas DJ, Taylor JA, Lavilla O, de la Cruz D, Neu J. Using machine learning analysis to assist in differentiating between necrotizing enterocolitis and spontaneous intestinal perforation: A novel predictive analytic tool. J Pediatr Surg. 2020 Nov 13: S0022-3468(20)30837-X. doi: 10.1016/j.jpedsurg.2020.11.008. Epub ahead of print.
17) Masi AC, Embleton ND, Lamb CA, Young G, Granger CL, Najera J, Smith DP, Hoffman KL, Petrosino JF, Bode L, Berrington JE, Stewart CJ. Human milk oligosaccharide DSLNT and gut microbiome in preterm infants predicts necrotising enterocolitis. Gut. 2020 Dec 16: gutjnl-2020-322771. doi: 10.1136/gutjnl-2020-322771. Epub ahead of print.
18) Rojas Beytía JP, J Cariaga Irarrázabal, F Castro Guerrero, P Domingo Carrasco, K Fernández Pérez, I Pavez Ortiz, NG Iturrieta Guaita, AM Silva Dreyer. [Health professional's perception about the use of human colostrum, as preventive measure for necrotizing enterocolitis in preterm newborns]. Rev Chil Pediatr 2020; 91: 536-544.
19) Liu L, L Liang, H Liang, M Wang, B Lu, M Xue, J Deng, Y Chen. Fusobacterium nucleatum Aggravates the Progression of Colitis by Regulating M1 Macrophage Polarization via AKT2 Pathway. Front Immunol 2019; 10: 1324.
20) Niemarkt HJ, TG De Meij, CJ Van Ganzewinkel, NKH De Boer, P Andriessen, MC Hütten, BW Kramer. Necrotizing Enterocolitis, Gut Microbiota, and Brain Development: Role of the Brain-Gut Axis. Neonatology 2019; 115: 423-431.
21) Raba AA, O'Sullivan A, Miletin J. Pathogenesis of necrotising enterocolitis: The impact of the altered gut microbiota and antibiotic exposure in preterm infants. Acta Paediatr 2021; 110: 433-440.
22) Liu H, XL Hong, TT Sun, XW Huang, JL Wang, H Xiong. Fusobacterium nucleatum exacerbates colitis by damaging epithelial barriers and inducing aberrant inflammation. J Dig Dis 2020; 21: 385-398.
23) Ng PC, KY Chan, KT Leung, YH Tam, TP Ma, HS Lam, HM Cheung, KH Lee, KF To, K Li. Comparative MiRNA Expressional Profiles and Molecular Networks in Human Small Bowel Tissues of Necrotizing Enterocolitis and Spontaneous Intestinal Perforation. PLoS One 2015; 10: e0135737.
24) Pu Z, M Xu, X Yuan, H Xie, J Zhao. Circular RNA circCUL3 Accelerates the Warburg Effect Progression of Gastric Cancer through Regulating

the STAT3/HK2 Axis. Mol Ther Nucleic Acids 2020; 22: 310-318.

25) Chen W, X Yan, T Tian, R Yan, X Wang, Z Yu, Y Li, L Zhang, S Han. Integrated analysis of a lncRNA-mRNA network reveals a potential mechanism underlying necrotizing enterocolitis. Mol Med Rep 2020; 22: 423-435.

26) Hong J, Guo F, Lu SY, Shen C, Ma D, Zhang X, Xie Y, Yan T, Yu T, Sun T, Qian Y, Zhong M, Chen J, Peng Y, Wang C, Zhou X, Liu J, Liu Q, Ma X, Chen YX, Chen H, Fang JY. F. nucleatum targets lncRNA ENO1-IT1 to promote glycolysis and oncogenesis in colorectal cancer. Gut. 2020 Dec 14:gutjnl-2020-322780. doi: 10.1136/gutjnl-2020-322780. Epub ahead of print.

27) Nolan LS, Parks OB, Good M. A Review of the Immunomodulating Components of Maternal Breast Milk and Protection Against Necrotizing Enterocolitis. Nutrients 2019; 12.

28) Pu Z, Y Liu, C Li, M Xu, H Xie, J Zhao. Using Network Pharmacology for Systematic Understanding of Geniposide in Ameliorating Inflammatory Responses in Colitis Through Suppression of NLRP3 Inflammasome in Macrophage by AMPK/Sirt1 Dependent Signaling. Am J Chin Med 2020; 48: 1693-1713.

29) Liu J, Q Yang, H Sun, X Wang, H Saiyin, H Zhang. The circ-AMOTL1/ENO1 Axis Implicated in the Tumorigenesis of OLP-Associated Oral Squamous Cell Carcinoma. Cancer management and research 2020; 12: 7219-7230.

30) Pandey SP, J Yan, JR Turner, C Abraham. Reducing IRF5 expression attenuates colitis in mice, but impairs the clearance of intestinal pathogens. Mucosal Immunol 2019; 12: 874-887.

31) Li P, H Lv, H Yang, JM Qian. IRF5, but not TLR4, DEFB1, or VDR, is associated with the risk of ulcerative colitis in a Han Chinese population. Scand J Gastroenterol 2013; 48: 1145-1151.

32) Yan J, SP Pandey, BJ Barnes, JR Turner, C Abraham. T Cell-Intrinsic IRF5 Regulates T Cell Signaling, Migration, and Differentiation and Promotes Intestinal Inflammation. Cell Rep 2020; 31: 107820.

33) Yang Y, Zhang C, Jing D, He H, Li X, Wang Y, Qin Y, Xiao X, Xiong H, Zhou G. IRF5 Acts as a Potential Therapeutic Marker in Inflammatory Bowel Diseases. Inflamm Bowel Dis 2021; 27: 407-417.

34) Fang H, Yang M, Pan Q, Jin HL, Li HF, Wang RR, Wang QY, Zhang JP. MicroRNA-22-3p alleviates spinal cord ischemia/reperfusion injury by modulating M2 macrophage polarization via IRF5. J Neurochem 2021; 156: 106-120.

35) Li H, J Sun, H Yang, X Han, X Luo, L Liao, B Yang, T Zhu, F Huo, W Guo, W Tian. Recruited CD68(+)CD206(+) macrophages orchestrate graft immune tolerance to prompt xenogeneic-dentin matrix-based tooth root regeneration. Bioact Mater 2021; 6: 1051-1072.

36) Ren CX, RX Leng, YG Fan, HF Pan, BZ Li, CH Wu, Q Wu, NN Wang, QR Xiong, XP Geng, DQ Ye. Intratumoral and peritumoral expression of CD68 and CD206 in hepatocellular carcinoma and their prognostic value. Oncol Rep 2017; 38: 886-898.

37) Park HJ, J Kim, FT Saima, KJ Rhee, S Hwang, MY Kim, SK Baik, YW Eom, HS Kim. Adipose-derived stem cells ameliorate colitis by suppression of inflammasome formation and regulation of M1-macrophage population through prostaglandin E2. Biochem Biophys Res Commun 2018; 498: 988-995.

38) Xie C, C Liu, B Wu, Y Lin, T Ma, H Xiong, Q Wang, Z Li, C Ma, Z Tu. Effects of IRF1 and IFN-β interaction on the M1 polarization of macrophages and its antitumor function. Int J Mol Med 2016; 38: 148-160.